JOURNAL OF SOLID STATE CHEMISTRY 92, 88—100 (1991)

Three-Dimensional/One-Dimensional Transition in the Cs^+ Sublattice of the Mixed Valence $CsTi_8O_{16}$ Hollandite: Structures at 297 and 673 K

E. FANCHON, J. L. HODEAU, J. VICAT, AND J. A. WATTS*

Laboratoire de Cristallographie, Centre National de la Recherche Scientifique, Laboratoire associé à l'Université J. Fourier, 166X, 38042 Grenoble Cedex, France

Received June 22, 1990; in revised form December 14, 1990

The mixed valence compound $Cs_xTi_8O_{16}$ has been studied by X-ray and electron diffraction. It was found to belong to the hollandite structural family, with a superstructure made of sharp peaks indicating a three-dimensional long range order of Cs cations at room temperature. Heating under the electron beam of a microscope induced a phase transition in which superstructure reflections transformed to a diffuse plane perpendicular to the tunnel direction of the hollandite structure. This was confirmed by a series of X-ray precession photographs taken at several temperatures: the transition temperature is about 593 K and the transition is reversible. X-ray structure analyses have been performed below the transition (at $T = 297$ K) and above it (at $T = 673$ K) and are reported in this paper. The space group of the high temperature phase is $I4/m$, with $a = 10.317(7)$ Å, $c = 2.980(1)$ Å. The superstructure at room temperature can be indexed in a supercell involving the multiplication of all three basic axes. The space group is $I4_1/a$, with $a = 14.524(11)$ Å, $c = 5.936(2)$ Å. At room temperature the two independent titanium sites have almost the same size, and the $3d$ electron is probably delocalized in accordance with the observation that $Cs_xTi_8O_{16}$ is a semiconductor. The phase transition is explained by the loss of lateral correlation among tunnels. No electronic phenomenon in the framework seems to be at the origin of the transition, which appears to be a purely ionic phenomenon.

Introduction

The general formula of hollandite compounds can be written $A_x^{u+}B_{8-y}^{v+}B_y'^{w+}O_{16}$ with $u = 1$ or 2, $v = 4$ or (rarely) 5 and $w = 1$, 2, or 3. Electroneutrality of course imposes $xu + (8 - y)v + yw = 32$. The generic hollandite structure has tetragonal space group $I4/m$ with a c axis on the order of 3 Å. Hollandites are constituted by a framework of $B/B'O_6$ octahedra providing *tunnels* of square cross-section running along the c axis (*1*). A tunnel can be viewed as a string of *cavities* large enough to accommodate the A cations. The distance between cavity centers is equal to the c cell parameter. The tunnel sites are only partially occupied and it is believed that the A cations can move within tunnels. Hollandites would thus be a perfect realization of one-dimensional ionic conductors. Indeed, an activation energy as low as 0.034 eV has been measured in $K_{1.54}Ti_{7.23}Mg_{0.77}O_{16}$ (*2*) for conductivity along the tunnels. Two adjacent cavities are separated by a bottleneck formed of four

* Division of Mineral Products, C.S.I.R.O., Melbourne, Australia.

oxygen atoms and the activation energy certainly depends on the relative size of the bottleneck and the mobile *A* cation for a given compound. A large number of oxides belonging to the hollandite family have been synthesized, showing that the structure tolerates various substitutions for the framework as well as the tunnel cations. One line of investigation is to study how the physical properties are influenced by the nature of the cations making up the hollandite structure.

Hollandite-type compounds generally display superstructure reflections or diffuse scattering in diffraction patterns. It is now well established that this is due to the arrangement of the *A* cations in the host lattice (*3—9*), although it has been found in two instances that the framework can create a superstructure of its own (*10, 11*). Two extreme cases of superstructure can be distinguished: a one-dimensional (1d) case in which the cations are ordered within tunnels (intratunnel order) with no correlation between tunnels; and a three-dimensional case (3d) in which there is both intra- and intertunnel ordering. Intermediate cases have been observed (*12, 13*) and can be characterized by a lateral correlation length. The 3d ordering is thus viewed as a *lateral* ordering of *chains* of cations, the 1d ordering being a prerequisite. This 1d order may be also of limited range and is characterized by an intratunnel correlation length. This length has been evaluated for example in $K_{1.54}Ti_{7.23}Mg_{0.77}O_{16}$ (*3*) from the width of diffuse planes to be about 35 Å. Another feature of the hollandite compounds is that the intratunnel order is often incommensurate with the period of the host lattice. With the 1d case being more common, only six X-ray single-crystal refinements of 3d hollandites have been reported so far: $Ba_{1.33}Mo_8O_{16}$ (*10*), $K_{1.8}Sb_{5.55}Li_{2.45}O_{16}$ (*14*), $Ba_{1.13}Ru_8O_{16}$ (*7*), $BaTi_6V_2O_{16}$ (*8*), $Ba_{1.2}Ti_{6.8}Mg_{1.2}O_{16}$ (*9*), $Ba_{1.33}Ti_{6.67}Mg_{1.33}O_{16}$ (*15, 16*).

$Cs_xTi_8O_{16}$ with $x \approx 1$ adopts the hollandite structure and its diffraction pattern exhibits a superstructure made of sharp peaks. The indexation of the diffraction pattern of $Cs_xTi_8O_{16}$ at room temperature requires a supercell built with all three basic axes, not only the tunnel axis *c*. To our knowledge, there is only one analogous hollandite structure, namely $BaTi_6V_2O_{16}$ (*8*). This compound is a mineral called mannardite, and the superstructure has been indexed in the same supercell. Another unusual feature is the low *occupation rate* κ of the tunnel cavities: the stoichiometry $x = 1$ corresponds to $\kappa = x/2 = \frac{1}{2}$, meaning that on average half of the cavities available for Cs cations in the tunnels are occupied. Such a low value is rare and has been found in $BaTi_8O_{16}$ (*17*) and in minerals for which the tunnels usually contain water molecules. To our knowledge, attempts to synthesize hollandites with $\kappa < \frac{1}{2}$ have been unsuccessful [see (*12*) for example]. However, metastable phases with $\kappa = 0$ and $\kappa = 0.24$ have been reported recently (*18*).

We report here on the existence in $Cs_xTi_8O_{16}$ of an order/disorder transition in which the 3d superstructure described above transforms to diffuse planes perpendicular to the tunnel axis as the temperature is raised. This transition is reversible and takes place at moderate temperatures, which made possible crystallographic studies below and above the transition temperature. The basic phenomenon involved is supposedly the increased mobility of Cs cations within tunnels at high temperature, leading to the loss of intertunnel order. It is the first report of an order/disorder phase transition in hollandite. Diffraction studies of $K_{1.5}Ti_{6.5}Al_{1.5}O_{16}$ (a 1d compound at room temperature) show that intra- and intertunnel correlation lengths increase with decreasing temperature (*19*), but the diffuse patterns do not condensate into sharp peaks down to 20 K.

Mixed-valence hollandites are qualitatively distinct from hollandites having two

different kinds of B/B' cations in the framework. For example the formation of tetranuclear *clusters* due to strong metal—metal bonds has been evidenced in two mixed-valence molybdenum compounds: $Ba_{1.33}Mo_8O_{16}$ (*10*) and $K_2Mo_8O_{16}$ (*11*). In the case of titanium compounds one may draw an analogy with the Magneli phases which are also constituted of rutile-like octahedra chains. In these compounds it has been established (*20*) that certain chains contain only Ti^{3+} cations while others contain only Ti^{4+} cations. This type of ordering induces differences in Ti—Ti bond lengths and can be observed by X-ray diffraction. We speculated that if a similar phenomenon is present in $Cs_xTi_8O_{16}$, it can participate in the 3d ordering of Cs atoms, and the 3d/1d transition described above may be accompanied or driven by an electronic change in the framework in which the *d* valence electrons become delocalized. The aim of this paper is to clarify the nature of the transition, in particular to determine whether the transition is a purely ionic phenomenon, or whether it has an electronic component.

Experimental

The samples used in this study have been synthesized by an electrochemical method (*21*). The same combination [$Cs,Ti^{4+}/Ti^{3+}$] has also been synthesized subsequently (*22, 23*), but with a different stoichiometry ($x = 1.33$).

The compound was first investigated by electron diffraction. This was performed using a Philips electron microscope (120 kV) equipped with a side-entry double tilt goniometer. Specimens were ground in an agate mortar and mounted on holey carbon films. The crystals have tetragonal symmetry. A superstructure formed of sharp peaks in the $l_{sub} = n/2$ (n odd) layers was observed (Fig. 1), and no diffuse scattering was visible (the subscript 'sub' identifies quantities expressed in the basic hollandite cell, or *subcell*). A phase transition was induced when the beam intensity was increased: the superstructure peaks elongate in the plane perpendicular to the c tetragonal axis and eventually become diffuse planes at the highest temperature attainable in this way (which was not known). Diminishing the beam intensity allows the recovery of the three-dimensional ordering, indicating that the transition is reversible. Additional experiments were performed on a precession camera equipped with a high temperature device (*24*). This device shows good temperature control (±2°C). The temperature was increased by 10° steps and the temperature was allowed to stabilize for 15 min before a precession picture was taken. The transition is continuous over the range of temperature 315—325°C. The same series of photographs taken while lowering the temperature confirms that the transition is reversible and does not reveal hysteresis. Both superstructures (sharp peaks and diffuse streaks) are commensurate with $l_{sub} = n/2$ (n odd). We have looked for the existence of this kind of transition in other hollandite-type compounds having three-dimensional order at room temperature. The results of this work will be reported elsewhere.

A long exposure (10 days) precession photograph was taken at 297 K to identify possible weak diffuse scattering. As shown in Fig. 2, diffuse planes are observed at $l_{sub} = 0.5$, indicating that the compound is not fully ordered.

The high temperature diffraction pattern has $I4/m$ symmetry, and is characteristic of the basic hollandite structure. The superstructure revealed by precession photographs at room temperature can be indexed in the following supercell: $a = a_{sub} + b_{sub}$, $b = a_{sub} - b_{sub}$, $c = 2c_{sub}$ (a_{sub}, b_{sub}, c_{sub} being the parameters of the subcell). The extinction observed on the $h0l$ and $0kl$ layers show systematic absences consistent with the space group $I4_1/a$. This is confirmed by photographs of the $hk0$, $hk1$ and $hk2$ layers

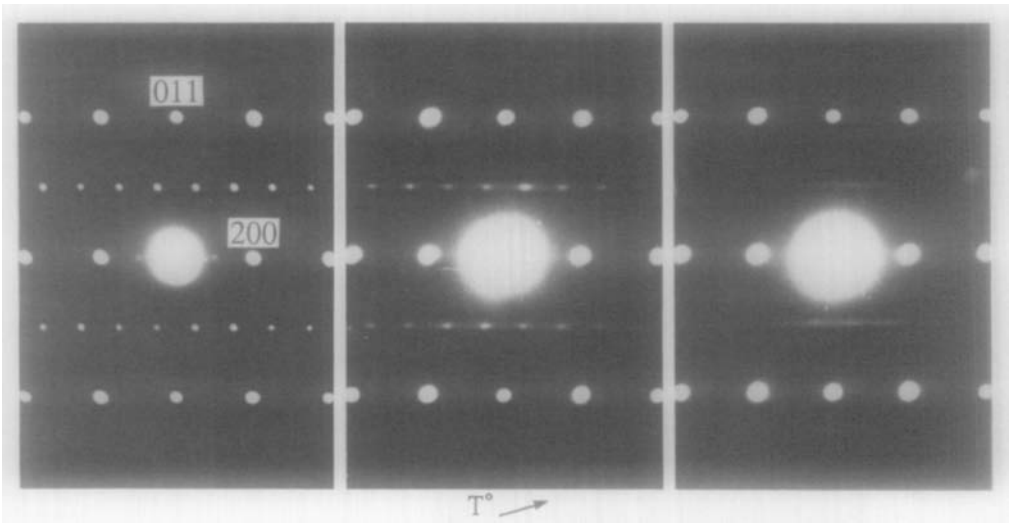

FIG. 1. [0 1 $\bar{1}$] electron diffraction pattern from $Cs_xTi_8O_{16}$. The transformation of the superstructure at $l_{sub} = \frac{1}{2}$ from sharp spots to diffuse streaks results from the heating obtained by increasing the electron beam intensity.

taken on the same sample with the De-Jong—Bouman method. The space group $\{I4_1/a; a, b, c\}$ is a subgroup of $\{I4/m; a_{sub}, b_{sub}, c_{sub}\}$ (*25*), which corresponds to the substructure.

The X-ray data collection at $T = 297$ K and at $T = 673$ K were both performed on a four-circle Philips PW1100 diffractometer with graphite monochromated Ag$K\alpha$ radiation. The lattice parameters listed in Table I were refined from θ values of 26 reflections over the range $20° \leq 2\theta \leq 44°$ determined with diffractometer centering routines. The background measuring time was equal to scan time and the intensities of three standard reflections were monitored every 2 hr. Other details are given in Table I.

Because of their weak intensities, no *superstructure* reflections were measured beyond $\theta = 20°$ at room temperature. All reflections in the $l = 1$ and $l = 3$ layers are superstructure reflections and were remeasured with better statistics: the maximum authorized number of scans was increased to 10, and the preset number of counts was set to 5000 and 10,000 for $l = 1$ and $l = 3$, respectively. The scan width was increased to 1.8° for measurements in the $l = 3$ layer. All other parameters are identical to the "main" data collection. No intensity test was performed after the first scan, so that all the reflections were measured. About 30 strong reflections showing a strong dissymmetry in the background counts were remeasured individually with a larger scan-width. A profile revealed that they were truncated. We also measured reflections along the (001) row for $-12 \leq l \leq 12$ in order to check the $l = 4n$ condition of presence.

The additional extinction rule $2h + l = 4n$ was observed during data collection. This corresponds to a special extinction of the space group observed when all the atoms are in special positions 4(*a*), 4(*b*) or 8(*e*), which is a priori not the case here. Rewriting this relation with the indices of the subcell gives: $h_{sub} + k_{sub} + l_{sub} = 2n$, which corresponds to a body-centered extinction *in the subcell*. We will come back to that point later.

The data set at T = 673 K was collected right after the room temperature set on the

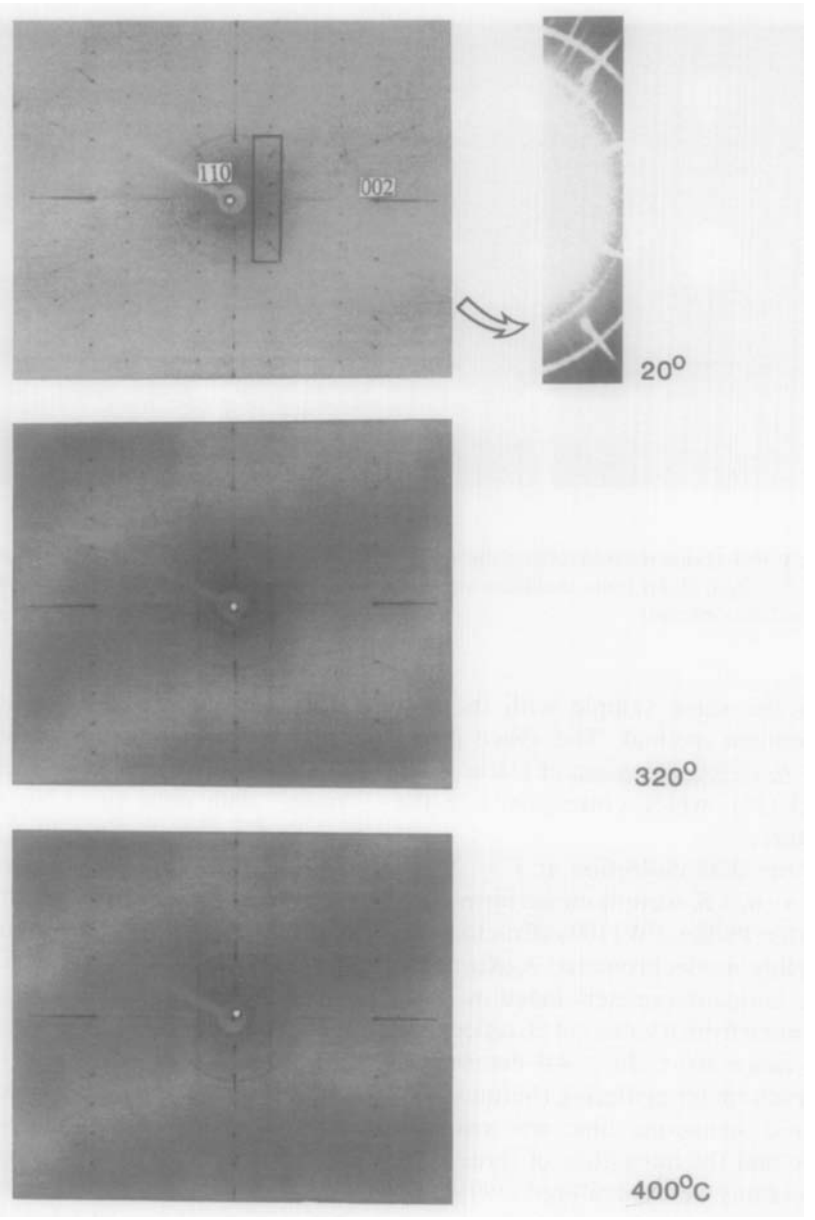

FIG. 2. X-ray precession photographs of $Cs_xTi_8O_{16}$ at three temperatures. The reciprocal plane is defined by $(a^*_{sub} + b^*_{sub}, c^*_{sub})$. The insert shows a 10-day precession exposure revealing a diffuse streak at $l_{sub} = \frac{1}{2}$.

same crystal, without dismounting it. The heating device used is the one (*24*) used in the precession experiments described above.

The Lorentz and polarization corrections were applied, as well as polyhedral absorption correction ($\mu = 40.98\ cm^{-1}$). The sample is delimited by five pairs of faces: (0 0 ±1), (0 ±1 0), (−1 1 0) and (1 −1 0), (±1 0 0), (1 0 0) and −1 −1 0) and the distances

TABLE I

SUMMARY OF CRYSTAL DATA, INTENSITY MEASUREMENTS, AND STRUCTURE REFINEMENT PARAMETERS

	T = 293 K	T = 673 K
1. *Crystal data*		
Space group	$I4_1/a$	$I4/m$
Cell dimensions (Å)	a = 14.524(11)	a = 10.317(7)
	c = 5.936(2)	c = 2.980(1)
Volume (Å^3)	V = 1252(1)	V = 317.2(3)
Z	4	1
2. *Intensity measurements*		
Radiation	Ag$K\alpha$	Ag$K\alpha$
Monochromator	Graphite	Graphite
Max θ	30°	30°
Scan mode	ω over $2 \leq \theta \leq 15°$ and $\theta/2\theta$ over $15 < \theta \leq 30°$	ω over $3 \leq \theta \leq 15°$ and $\theta/2\theta$ over $15 < \theta \leq 30°$
Scan width	$\Delta\theta(\theta_0)$ = 1.2°	$\Delta\theta(\theta_0)$ = 1.4°
Counter aperture		
Vertical edges	2°	2°
Horizontal edges	1.5°	1.5°
Scan speed	0.06° s^{-1}	0.06° s^{-1}
Preset number of counts	5000	5000
Maximum number of scans	4	4
3. *Data reduction*		
No. of reflections	4488	1598
R_{sym}[a]	3.6%	2.7%
No. of unique reflections	851	342
4. *Refinement*		
No. of refined parameters	61	24
Final R, R_w (%)[b]	5.9, 3.0	10.9, 5.0
$(\text{shift}/\sigma)_{max}$	0.8	0.7

[a] $R_{sym} = \{\Sigma_h\Sigma_i|\langle F(h)\rangle - F(h_i)|\}/\Sigma_h\Sigma_i F(h_i)$, with $\langle F(h)\rangle$ = average of equivalent reflections h_i.
[b] $R = \{\Sigma(F_{obs} - F_{calc})^2/\Sigma F_{obs}^2\}^{1/2}$, $R_w = \{\Sigma w(F_{obs} - F_{calc})^2/\Sigma w F_{obs}^2\}^{1/2}$ (weighting scheme defined in text).

(mm) between the faces of a given pair are: 0.14, 0.06, 0.07, 0.06, 0.05, respectively.

Structure Determination and Refinement

297-K Structure

Initial positions of the framework atoms were deduced from the basic hollandite structure (*26*) by applying the following transformation:

$$x = (x_{sub} + y_{sub})/2$$

$$y = (-x_{sub} + y_{sub})/2 + \tfrac{1}{2}$$

$$z = z_{sub}/2.$$

We have chosen origin choice No. 1 (*25*), because the $\bar{4}$ axis which corresponds to the tunnel axis is then going through the origin according to the usual representation. The stoichiometry of the compound indicates that four Cs atoms are present in the supercell so that these cations have to occupy positions 4(*a*) or 4(*b*) if they are ordered. The $b/2$ translation in the above transformation was applied for these special positions to correspond to the cavity center instead of the bottleneck.

The multiplicity of the general position in $I4_1/a$ is twice that of $I4/m$, but the volume of the supercell is four times that of the basic

cell, so that a second set of independent atoms is needed. This was obtained by remarking that the symmetry center which was in ($\frac{1}{2}$ 0 0) in the subcell has no counterpart in $I4_1/a$. Framework atoms are labeled with two characters: the figure indicates the number of the subcell atom from which the position derives, and the letter identifies the set: *a* for first set and *b* for second set.

Refinement was initiated with one Cs placed on special site 4(*a*). The other special position 4(*b*) provides an equivalent starting point for refinement since the framework is initially undistorted. The tunnel sequence generated by the symmetry is a Cs-vacancy and corresponds to the doubling of the *c* axis. The refinement of this initial model with 851 independent observations leads to high values of the crystallographic indices: R_w = 20.6%, R = 22.1% with 58 refined parameters (the thermal parameters of the framework atoms are anisotropic). A Fourier synthesis brings out a peak of electronic density in the tunnels at (0 0 $\frac{1}{2}$). This lead us to include an additional Cs on site 4(*b*) and to refine fractional occupancies *p*[Cs(1)] and *p*[Cs(2)]. This gives a better agreement but it is still not satisfactory. Two additional sites were added: Cs(3) at (0 0 $\pm\delta z_3$) and Cs(4) at (0 0 $\frac{1}{2}\pm\delta z_4$). Five parameters are added in this process: two displacements, two populations, and one isotropic thermal parameter applied to both sites. The results are now satisfactory, but severe correlations are noticed between *p*[Cs(1)] and *p*[Cs(3)] on one hand, and between *p*[Cs(4)] and *p*[Cs(4)] on the other hand. The stoichiometry $x = 2\kappa$ nevertheless refines to 1.06.

The off center sites Cs(3) and Cs(4) probably result from the occupation of two *contiguous* cavities along the tunnel axis. This is consistent with the refined occupation rate κ being greater than $\frac{1}{2}$. This interpretation implies that the two shifted sites have the same population, so that the constraint *p*[Cs(3)] = *p*[Cs(4)] was introduced in the refinement. Additional constraints between isotropic thermal factors (U[Cs(1)] = U[Cs(2)] and U[Cs(3)] = U[Cs(4)]) were also imposed. The agreement factors are now R_w = 3.0%, R = 5.9% with 61 refined parameters. A refinement with anisotropic thermal factors for Cs is not possible because the correlations between these parameters and the populations are too strong. The final atomic parameters and the main interatomic distances are listed in Tables II and III, respectively. The reason of the special extinction $2h + l = 4n$ (with subcell indices) is now clear: the Cs partial structure obeys this extinction because these atoms are on

TABLE II

STRUCTURE OF $Cs_xTi_8O_{16}$ AT T = 297 K. ATOMIC COORDINATES AND ISOTROPIC (FOR Cs) OR EQUIVALENT (FOR Ti AND O) THERMAL FACTORS (Å^2) ($U_{eq} = \frac{1}{3}\Sigma_i U_{ii}$) (e.s.d.'s ARE GIVEN IN PARENTHESES)

	x	y	z	U_{eq}/U_{iso}
Cs(1)	0	0	0	0.0090(4)
Cs(2)	0	0	$\frac{1}{2}$	U[Cs(1)]
Cs(3)	0	0	0.059(1)	0.0110(8)
Cs(4)	0	0	0.558(1)	U[Cs(3)]
Ti(1*a*)	0.25813(7)	0.40887(6)	−0.00368(32)	0.0084(3)
Ti(1*b*)	0.24368(7)	0.09203(6)	−0.00418(32)	0.0080(3)
O(1*a*)	0.1834(2)	0.5257(2)	−0.0048(12)	0.0073(12)
O(2*a*)	0.3517(2)	0.3134(2)	0.0041(12)	0.0067(10)
O(1*b*)	0.3168(2)	−0.0253(2)	−0.0042(12)	0.0087(10)
O(2*b*)	0.1479(2)	0.1857(2)	0.0025(12)	0.0085(10)

Note. Fractional occupancies for Cs: *p*[Cs(1)] = 0.509(8), *p*[Cs(2)] = 0.148(7), *p*[Cs(3)] = *p*[Cs(4)] = 0.101(4), which gives x = 1.062(3).

TABLE III

STRUCTURE OF $Cs_xTi_8O_{16}$ AT T = 297 K. INTERATOMIC DISTANCES (Å) (e.s.d.'s ARE GIVEN IN PARENTHESES)

Cs(3)—Cs(4)	3.663(12)		Cs(1)—Cs(1)	5.936(2)	
Cs(1)—O(1*a*)	3.086(5)	×4	Cs(2)—O(1*a*)	3.058(6)	×4
Cs(1)—O(1*b*)	3.057(5)	×4	Cs(2)—O(1*b*)	3.081(6)	×4
Cs(1)—O(2*b*)	3.448(6)	×4	Cs(2)—O(2*a*)	3.462(6)	×4
Ti(1*a*)—Ti(1*b*)	2.971(3)		Ti(1*a*)—Ti(1*b*)	2.965(3)	
Ti(1*a*)—O(1*a*)	2.014(4)		Ti(1*b*)—O(1*b*)	2.008(4)	
Ti(1*a*)—O(2*a*)	1.942(4)		Ti(1*b*)—O(2*b*)	1.946(4)	
Ti(1*a*)—O(1*a*)	1.918(6)		Ti(1*b*)—O(1*a*)	2.014(6)	
Ti(1*a*)—O(1*b*)	1.996(6)		Ti(1*b*)—O(2*a*)	2.011(6)	
Ti(1*a*)—O(2*b*)	2.025(6)		Ti(1*b*)—O(2*b*)	1.949(6)	
Ti(1*a*)—O(2*a*)	1.959(6)		Ti(1*b*)—O(1*b*)	1.941(6)	
Average	1.976		Average	1.978	
Distortion	$3.8\ 10^{-4}$		Distortion	$2.8\ 10^{-4}$	

TABLE IV

STRUCTURE OF $Cs_xTi_8O_{16}$ AT $T = 673$ K. ATOMIC COORDINATES AND THERMAL FACTORS (Å^2) ($U_{eq} = \frac{1}{3}\Sigma_i U_{ii}$) IN THE SUBCELL (e.s.d.'s ARE GIVEN IN PARENTHESES)

	x	y	z	U_{eq}
Cs(1)	0	0	$\frac{1}{2}$	0.0436(12)
Ti(1)	0.3491(2)	0.1659(2)	0	0.0137(4)
O(1)	0.1583(8)	0.2078(8)	0	0.017(2)
O(2)	0.5383(8)	0.1649(8)	0	0.019(2)

special sites 4(*a*), 4(*b*), or 8(*e*), and the average framework is body-centered in the subcell so that only distortion of the framework can break this extinction rule.

673-K Structure

There are no superstructure *peaks* at 673 K and the initial parameters are simply those of $K_{1.33}Mn_8O_{16}$ (*26*). The refined anisotropic thermal parameters of Cs reveal that the vibration along the tunnel axis is very large ($U_{11} = U_{22} = 0.0216(8)$ Å^2 and $U_{33} = 0.0875$ (*35*) Å^2). The refinement of the occupancy leads to $x = 1.10(1)$ in agreement with the room temperature value. The crystallographic R factors are $R_w = 5.0\%$, $R = 10.9\%$ with 24 refined parameters and 342 observations. An attempt of refinement with split sites gives the same R factors. The final atomic parameters and the main interatomic distances are listed in Tables IV and V.

TABLE V

STRUCTURE OF $Cs_xTi_8O_{16}$ AT $T = 673$ K. INTERATOMIC DISTANCES (Å) (e.s.d.'s ARE GIVEN IN PARENTHESES)

Cs—O(1)	3.082(7)	×8	Ti—O(1)	2.018(9)	
			Ti—O(1)	1.979(6)	×2
Cs—O(2)	3.485(9)	×4	Ti—O(2)	1.953(9)	
			Ti—O(2)	1.991(6)	×2
Ti(1)—Ti(1)	2.980(3)		Average	1.985	
			Distortion	0.9 10^{-4}	

All refinements reported here are based on F with $1/\sigma(F)^2$ weighting scheme (where σ is due to the counting statistics). The software packages used are MXD (*27*) for the 297-K structure, and SDP (*28*) for the 673-K structure.

Discussion

The cell parameters can be compared with other mixed-valence titanium hollandites. The values are

$Ba_{1.16}Ti_8O_{16}$	$a = 10.106$ Å	$c = 2.964$ Å (*29*),
$K_{0.48}Ti_8O_{16}$	$a = 10.182$ Å	$c = 2.966$ Å (*18*),
$K_{1.35}Ti_8O_{16}$	$a = 10.188$ Å	$c = 2.966$ Å (*30*),
$Cs_{1.06}Ti_8O_{16}$ ($T = 297$ K, basic cell)	$a = 10.270$ Å	$c = 2.968$ Å.

This reveals that the a parameter increases with the ionic radius of the tunnel cation, whereas the c axis is mostly constant. In comparison the cell variation with temperature is quite important ($\Delta a = 0.047$ Å, $\Delta c = 0.012$ Å), and the expansion is essentially isotropic. We previously found (*26*) by analyzing data on several structures reported in the literature that the cell parameters depend very little on the A ionic radius, but mainly depend on the average ionic radius of B and B'. This does not account for the effect of such large ions as Cs^+, nor for the effect of temperature.

The basic structural unit forming the framework is the double chain of edge-sharing BO_6 octahedra. Four double chains assemble by corner sharing to create square tunnels. There are two crystallographically independent octahedra in the room temperature structure. As expected, the four shared octahedral edges are significantly shortened. The average Ti—O distances for the two independent octahedra are 1.976 and 1.978 Å, in agreement with the ionic radius sum (*31*) $\langle r(Ti^{4+}/Ti^{3+})\rangle + r(O^{2-}) = 1.99$. These distances are shorter than the ones found in monoclinic $BaTi_8O_{16}$: 1.985 Å (*17*). Interestingly, this value corresponds to

what we find for the 1d phase (at 673 K). The octahedral distortion as defined by Shannon (*31*) is rather low: 3.9×10^{-4} and 2.8×10^{-4}, compared with the average distortion observed in $Ba_{1.33}Ti_{6.67}Mg_{1.33}O_{16}$ (*16*): 7.2×10^{-4}. This shows that no octahedral distortion is required in order to accommodate the large Cs^+ cations in the tunnel cavities. The Ti cations are displaced with respect to the center of gravity of the octahedra: 0.102 Å for Ti(1*a*) and 0.115 Å for Ti(1*b*). Similar displacements have been found in other hollandites: 0.14 Å in $Ba_{1.33}Ti_{6.67}Mg_{1.33}O_{16}$ (*16*), 0.13 Å in $Ba_{1.14}Ti_{5.72}Al_{2.28}O_{16}$ (*32*).

The two titanium-site sizes as measured by the Ti—O distances are almost the same. This shows that there is no preferential occupation of one site by the *d* valence electrons. The Ti^{3+} valence electron is probably delocalized, which is consistent with the fact that $Cs_xTi_8O_{16}$ is a semiconductor (*21*). The shorter Ti—Ti distances are those linking atoms within a chain of octahedra. They are larger than 2.965 Å, ruling out the possibility of metal—metal bonding. Referring to our hypothesis in the introduction, the answer is that no electronic phenomenon seems involved in the triggering of the phase transition. The framework contributes to the superstructure reflections only through passive displacements accompanying the Cs ordering. The most noticeable of these is the Ti shift mentioned previously.

Cs^+ is the biggest cation that can be accommodated in the hollandite structure. The cesium atoms are in a slightly distorted square-prismatic environment formed by oxygen atoms. The centered Cs(1) atom gives Cs—O distances of 3.08 Å, and is thus in contact with the eight oxygen atoms according to the sum of ionic radii $r(Cs^+) + r(O^{2-}) = 3.12$ Å. These oxygen atoms are not in contact with each other, the shortest O—O distance being the vertical edges of the square-prism at 2.905 Å, which is much larger than $2r(O^{2-}) \approx 2.5$ Å. The cavity corresponding to an "empty" site has the same horizontal dimensions due to symmetry, but slightly longer vertical edges: 2.972 Å. It should be noted however, that this cavity is partially occupied due to disorder as discussed below.

The off-center sites are 0.350 Å away from this cavity center. This shift has been evaluated (from rotation photographs) to be about 0.12 c_{sub} in $Cs_{1.33}Ti_{7.33}Mg_{0.67}O_{16}$ (*22*). Although the occupation rate is lower and the *B'* cation is different, we find the same value for the refined structure of $Cs_xTi_8O_{16}$. It is however difficult to understand how this shift is accommodated since the centered Cs are already in contact with the eight neighboring oxygens. The structural study of the $x = 1.33$ compound would certainly provide an answer to this question because in that case *all* the Cs cations are on off-center sites. In the current compound these off-center sites are only partially occupied and we observe a framework averaged over the disorder.

Bond-strength calculations based on the Brown and Wu method (*33*) have been made assuming a fully ordered structure. The calculated valences are -2.04, -1.93, -2.04, -1.99 for the oxygen atoms, and 3.81, 3.78 for the Ti^{4+}/Ti^{3+} hybrid cation, showing that there is good charge balance in the framework. The Cs valence obtained by this method is 1.63, which is grossly overestimated and indicates that significant interactions have not been accounted for. These can most certainly be identified as being the Cs—Cs intratunnel repulsive interactions.

The intratunnel order is based on the [Cs − 0] sequence (0 represents a vacancy). In other words Cs occupy every other cavity along the tunnel axis, as expected from the stoichiometry. In most 3d hollandite, the lateral arrangement of chains is such that vacancies are grouped in corrugated sheets (*12*). A corrugated sheet is best described by a pair of planes both perpendicular to the tunnel axis, with the distance between planes being $c_{sub}/2$. It is easy to check that

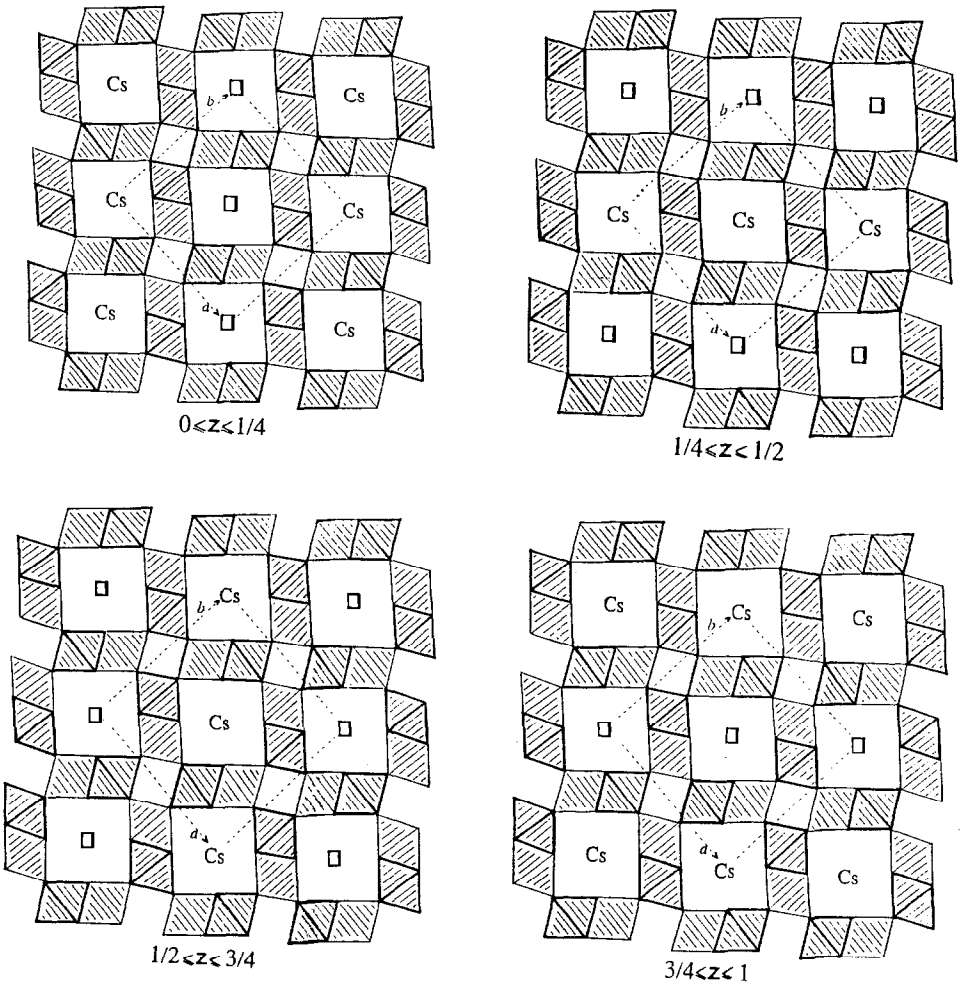

FIG. 3. View of the Cs-vacancy distribution down the c axis. Four different slices each $c_{sub}/2$ thick are represented. In the "corrugated sheet" type of distribution, two of these would be vacancy-only and the other two Cs-only.

every such pair of planes contains both cesium atoms and vacancies (Fig. 3) and that there is consequently no corrugated sheet of vacancies in $Cs_xTi_8O_{16}$ ($x \approx 1$). Instead, the distribution of charges is homogeneous. The mineral $BaTi_6V_2O_{16}$ (*8*), which has a similar tunnel occupation rate, adopts exactly the same distribution of Ba^{2+} cations (same space group $I4_1/a$). It should be noted that in both cases a lateral arrangement with corrugated sheets of vacancies is possible in space group $I4/m$ with supercell (a_{sub}, b_{sub}, $2c_{sub}$). A third example of compound where the vacancies are homogeneously distributed is $K_{1.33}Sb_{4.89}Mg_{3.11}O_{16}$ (*6*). It is interesting to note that this kind of distribution is not special to the $\kappa = \frac{1}{2}$ tunnel occupancy. The parameters controlling the *type* of lateral arrangement are not known.

As mentioned earlier the occurrence of off-center Cs positions can be explained by the existence of {Cs—Cs} defects in the nor-

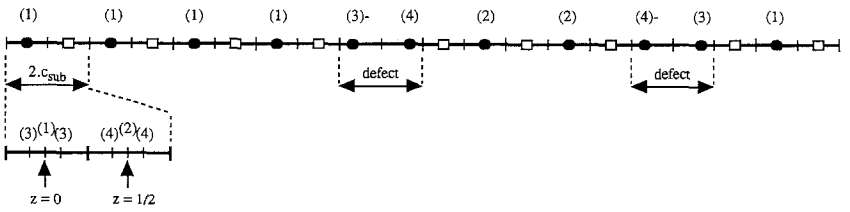

FIG. 4. Cs-vacancy ordering scheme. The number in parentheses refers to the crystallographic site (the minus sign indicates the symmetry-related site $00\bar{z}$). This stretch corresponds to the following occupancies: p[Cs(1)] = 0.5, p[Cs(2)] = 0.2, p[Cs(3)] = p[Cs(4)] = 0.1. This gives x = 1.10.

mal [Cs − 0] sequence. Figure 4 shows an attempt to rationalize the pattern of Cs site occupancies. Starting from the left one finds four times the reference motif [Cs − 0] corresponding to the occupation of site Cs(1). Then one {Cs—Cs} defect is encountered, after which the normal sequence resumes but is translated with respect to the reference sequence. This stretch of translated sequence corresponds to the occupation of site Cs(2). Finally a second defect translates back to the reference sequence. In this example there are 11 cations over 20 cavities (leading to κ = 0.55, x = 1.10), instead of 10 cations in the case of perfect order (leading to κ = 0.50, x = 1.00). The whole sequence reproduces approximately the pattern of occupancy values obtained in the refinement since there are five cations on Cs(1), 2 on Cs(2), 1 on Cs(3), and 1 on Cs(4), corresponding to the following occupancies: 0.5, 0.2, 0.1, 0.1, respectively. If the length of the translated sequence is reduced from $5c_{sub}$ to $3c_{sub}$ these values become 0.6, 0.1, 0.1, 0.1. Thus an equal random mixture of the two kinds of model would give 0.55, 0.15, 0.1, 0.1, and the average length of the translated sequence would be $4c_{sub}$. This value however should be taken with caution since p[Cs(1)] and p[Cs(2)] were correlated in the refinement, so that the ratio of translated sequence to reference is uncertain.

Another question is whether the defects are grouped in planes perpendicular to the tunnel axis or whether they are isolated. The first case corresponds to a microdomain model that has been developed for the $Ba_xTi_{8-x}Mg_xO_{16}$ ($1.1 < x < 1.33$) series. The existence of a weak diffuse plane at $l_{sub} = \frac{1}{2}$ superimposed to the superstructure reflections favors the second hypothesis. The coexistence of sharp superstructure peaks and diffuse planes at $l_{sub} = \frac{1}{2}$ has also been observed in $BaTi_6V_2O_{16}$ (*8*), $Ba_{1.14}Ti_8O_{16}$ (*33*), and some samples of $Cs_{1.32}Ti_8O_{16}$ (*33*).

Mijlhoff *et al.* (*12*) have developed a model in which the distribution of A cations within tunnels is described by a periodic modulation wave with square shape. The wavevector q is determined by the occupation rate of the tunnels and its value is 0.47 c^*_{sub} for x = 1.06, meaning that the superstructure is incommensurate with the period of the average framework. It is clear from our precession photographs that the room temperature superstructure is commensurate with q = 0.50. This indicates that there is no intratunnel order between the {Cs—Cs} sequence defects, whereas in the occupation wave model the occurrence of Cs—Cs pairs is dictated by the wave and thus gives rise to a strictly ordered (although incommensurate) pattern of defects.

The 673-K structure is more symmetric and there is only 1 independent octahedron. The average Ti—O bond is larger than the two room temperature values, and the distortion is smaller. An interesting result is that the Ti shift from the octahedron center is 0.10 Å. Cheary *et al.* (*32*) proposed that

lateral ordering of *A* chains could be determined by the framework polarizability arising from the off-centering of octahedral cations. They observed in several compounds that the smaller the off-center shift, the larger the lateral coherence length. Their interpretation is that a large shift implies a substantial screening of the intertunnel interaction, thus favoring 1d order. Other authors (*33*) proposed the same idea of framework screening, but based on the *electronic* polarizability of the framework cations. We think that an important conclusion to be drawn from the existence of a 3d/1d transition is that the state of order does not depend only on *static* structural features, and that dynamic aspects must be included in the description. This changes the nature of the problem into determining which parameters control the 3d—1d transition temperature.

It is clear that the transformation of sharp peaks into diffuse planes is due to the loss of lateral correlation among tunnels. This implies that above T_c the Cs^+ cations are able to hop from one cavity to another. Two adjacent cavities along the tunnel are separated by four oxygens at mid distance. The diagonal of this oxygen "square" minus twice the ionic radius $r(O^{2-})$ defines the bottleneck size, which is 2.89 Å at room temperature and 2.91 Å at $T = 673$ K. It is thus smaller than $2r(Cs^+) = 3.76$ Å by 0.87 Å (0.85 Å at $T = 673$ K) and should prevent the *A* cations from moving along the tunnels. We propose the following model to explain the Cs^+ mobility within tunnels. A vibrational mode of the framework may be associated with a "breathing" of the bottleneck, allowing the Cs cations to go across the bottleneck. Above a certain temperature this vibration mode could become more populated and the probability for a Cs^+ to hop from one cavity to another would increase dramatically. It is likely that the same transition exists for $Cs_{1.33}Ti_8O_{16}$, possibly with a lower transition temperature. The mixed-valence character of the framework may also be a factor influencing the transition temperature.

References

1. A. Byström and A. M. Byström, *Acta Crystallogr.* **3,** 146 (1950).
2. S. K. Khanna, G. Grüner, R. Orbach, and H. U. Beyeler, *Phys. Rev. Lett.* **47,** 255 (1981).
3. H. U. Beyeler, *Phys. Rev. Lett.* **37,** 1557 (1976).
4. L.A. Bursill and G. Grzinic, *Acta Crystallogr. Sect. B* **36,** 2902 (1980).
5. J. E. Post, R. B. Von Dreele, and P. R. Buseck, *Acta Crystallogr. Sect. B* **38,** 1056 (1982).
6. A. Pring, D. J. Smith, and A. D. Jefferson, *J. Solid State Chem.* **46,** 373 (1983).
7. C. C. Torardi, *Mater. Res. Bull.* **20,** 705 (1985).
8. J. T. Szymanski, *Canad. Mineral.* **24,** 67 (1986).
9. E. Fanchon, J. Vicat, J.-L. Hodeau, P. Wolfers, D. Tran Qui, and P. Strobel, *Acta Crystallogr. Sect. B* **43,** 440 (1987).
10. C. C. Torardi and R. E. McCarley, *J. Solid State Chem.* **37,** 393 (1981).
11. C. C. Torardi and J. C. Calabrese, *Inorg. Chem.* **23,** 3281 (1984).
12. F. C. Mijlhoff, D. J. IJdo, and H. W. Zandbergen, *Acta Crystallogr. Sect. B* **41,** 98 (1985).
13. H. W. Zandbergen, P. L. A. Everstijn, F. C. Mijlhoff, G. H. Renes, and D. J. W. IJdo, *Mater. Res. Bull.* **22,** 431 (1987).
14. H. Watelet, J.-P. Besse, G. Baud, and R. Chevalier, *Mater. Res. Bull.* **17,** 863 (1982).
15. E. Fanchon, J. Vicat, J.-L.Hodeau, J.-P. Lévy, and P. Wolfers, *Acta Crystallogr. Sect. A* **43**(Suppl.), C-129 (1987).
16. E. Fanchon, J. Vicat, J.-L. Hodeau, and P. Wolfers, in preparation (1990).
17. J.Schmachtel and Hk. Müller-Buschbaum, *Z. Naturforsch.* **35b,** 332 (1980).
18. M. Latroche, L. Brohan, R. Marchand, and M. Tournoux, *J. Solid State Chem.* **81,** 78 (1989).
19. H. Terauchi, T. Futamura, T. Ishii, and Y. Fujiki, *J. Phys. Soc. Japan* **53,** 2311 (1984).
20. M. Marezio, D. B. McWhan, P. D. Dernier, and J. P. Remeika, *Phys. Rev. Lett.* **28,** 1390 (1972).
21. A. F. Reid and J. A. Watts, *J. Solid State Chem.* **1,** 310 (1970).
22. H. U. Beyeler and C. Schüler, *Solid State Ionics* **1,** 77 (1980).

23. S. E. KESSON AND T. J. WHITE, *Proc. R. Soc. London A* **405,** 73 (1986).
24. R. ARGOUD AND J.-J. CAPPONI, *J. Appl. Crystallogr.* **17,** 420 (1984).
25. "International Tables for Crystallography," (T. Hahn, Ed.), Vol. A, Reidel, Dordrecht/Boston (1983).
26. J. VICAT, E. FANCHON, P. STROBEL, AND D. TRAN QUI, *Acta. Crystallogr. Sect. B* **42,** 162 (1986).
27. P. WOLFERS, *J. Appl. Cryst.* **23,** 554 (1990).
28. B. FRENZ, "Enraf-Nonius Structure Determination Package," Delft Univ. Press, Delft, Holland (1982).
29. E. FANCHON, J. VICAT, J.-L. HODEAU, P. STROBEL, AND J. P. LÉVY, in preparation (1990).
30. T. VOGT, E. SCHWEDA, C. WÜSTEFELD, J. STRÄHLE, AND A. K. CHEETHAM, *J. Solid State Chem.* **83,** 61 (1989).
31. R. D. SHANNON, *Acta Crystallogr. Sect. A* **32,** 751 (1976).
32. R. W. CHEARY AND R. SQUADRITO, *Acta Crystallogr. Sect. B* **45,** 205 (1989).
33. S. E. KESSON AND T. J. WHITE, *Proc. R. Soc. Lond. A* **408,** 295 (1986).
34. I. D. BROWN AND K. K. WU, *Acta Crystallogr. Sect. B* **32,** 1957 (1976).